Absolute determination of molecular-beam intensities

Klaus Kern, Bernd Lindenau, Rudolf David, and George Comsa

Institut für Grenzflächenforschung und Vakuumphysik, Kernforschungsanlage Jülich GmbH, Postfach 1913, D-5170 Jülich, West Germany

(Received 6 August 1984; accepted for publication 29 August 1984)

A new type of detector for the determination of absolute molecular-beam intensities is described. The intensity is obtained from the work done on a cylindrical rotating body by the torque exerted by the impinging beam particles. The detector takes advantage of the very low and constant bearing friction of magnetically suspended rotors and of the complete particle momentum accommodation on uncleaned surfaces. The detection limit of the present design is $I_0^{\min} = 1.2\times10^{15}/M\tilde{v}$, where M is the atom mass and $\tilde{v}$ the average velocity of the beam particles in ms^{-1}. The molecular-beam detector turns out to be an absolute instrument. Principle, experimental performance, and measurements with helium nozzle beams are reported.

INTRODUCTION

Supersonic nozzle beams obtained by expansion of gas under high pressure through sonic throats are widely used in atomic, molecular, and surface physics. The narrow velocity distribution and the high center-line intensity are the basic features which make nozzle beams so attractive. The exact knowledge of both velocity distribution and intensity is of obvious importance. The velocity distribution parallel to the streamlines has been intensively studied during the past two decades and highly accurate time-of-flight results are available. Absolute center-line-intensity data are, however, scarce.

Over the years a large number of techniques have been developed to detect molecular beams. None of these detectors is an absolute instrument, i.e., they need calibration. The calibration has inherent disadvantages. For example, the most widespread detector, based on electron bombardment ionization, is calibrated under isotropic conditions, which is often questionable. Difficulties with the bolometer calibration result from the poor energy accommodation of many interesting gases.[1] Energy accommodation depends on the actual condition of the bolometer surface. Detection systems based on the measurement of transferred normal momentum, as Becker's capacitance-type manometer (baratron)[2] or Choi's microphone detector[3] are affected by hysteresis. An advantageous alternative, where calibration under isotropic conditions is unproblematic, are the flux detectors of the Pitot type. However, pumping and degassing due to the low conductance which connects the gauge volume with the system may cause trouble.

Here we report on the development of an absolute momentum flux detector, i.e., a detector which needs no calibration. The instrument makes full use of the directionality of the momentum flux. It is suited for measurements with beams of molecules of any kind. The principle is the deceleration (or acceleration) of a freely spinning rotor caused by tangential momentum transfer due to impinging beam molecules. The technique takes full advantage of the low bearing friction of magnetically suspended rotors. Momentum accommodation of randomly incident molecules has been examined in the past.[4–11] It was found that, within a few percent, momentum accommodation at technical metal surfaces is complete for all examined gases. As will be shown below, scattering of molecular beams from technical metal surfaces is almost diffuse, i.e., the tangential momentum exchange is also almost perfect. For this reason the molecular-beam momentum flux may be calculated from the work done on the rotor by the impinging beam particles using only the rotor material density and its geometrical shape. In conjunction with the known mean velocity of the beam particles, absolute intensity data can be evaluated.

In the following sections the theoretical background of the instrument, the experimental performance, and a set of results on absolute intensity data of highly expanded helium-free jets are presented.

I. PRINCIPLE

The basic assumption for the realization of an absolute momentum flux detector is the almost perfect accommodation of momentum. If the flux of molecules leaving a surface is symmetric with respect to the surface normal, accommodation of tangential momentum is perfect (the molecules have "forgotten" their incident direction). As will be shown below (Sec. III) the angular distribution of beam molecules reemitted from technical metal surfaces is, indeed, almost symmetric with respect to the surface normal. Perfect accommodation of tangential momentum is assumed in Secs. I and II, and demonstrated *à posteriori* in Sec. III.

A molecular beam impinging on a surface exerts a very small force. Typical magnitudes for the particle flux used in the present study (thermal helium nozzle beam, $T_0 = 300$ K, $\tilde{v}\approx1770$ ms^{-1}, $m = 6.65\times10^{-27}$ kg, beam divergence of 0.09°) are: flux $I_0\sim10^{13}$ particles s^{-1} and a resulting momentum flux (force) $\sim10^{-10}$ N.

An obvious way to measure the tangential momentum transfer is the torsion pendulum [Fig. 1(a)]. The sensitivity of this device is ultimately limited by the smallest diameter of the filament, which is still capable of sustaining the disk weight. Minimum detectable forces of the order $\sim10^{-13}$ N and below can in principle be achieved.[12] However, requirements like compact dimensions, insensitivity to shock and vibration, and reliable and adequate evaluation of the mea-

 0034-6748/85/010052-06$01.30

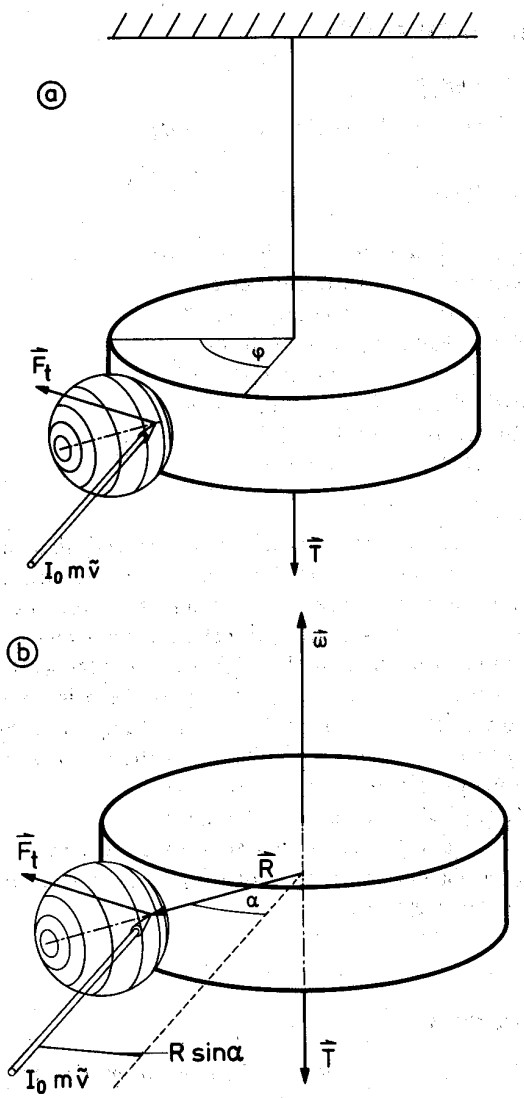

FIG. 1. (a) Torsion pendulum as momentum flux detector. (b) Freely rotating disk as momentum flux detector: (α) angle of incidence, ($\vec{\omega}$) angular velocity, ($\vec{R}$) disk radius, ($\vec{F}_t$) the tangential force, ($\vec{T}$) the resulting torque.

surable variable are hardly met. In addition, the device is still subject to calibration.

The torsion pendulum is in fact a static indicator for a force acting tangentially on the disk. Let us assume that the pendulum disk is suspended by fields and not by a material filament. The tangentially acting force now brings the disk into rotation [Fig. 1(b)], i.e., the force does work on the disk. The amount of work done during a given time interval is obtained from the rotation frequency change. The method becomes an integral method; its sensitivity increases with the measuring time. Moreover, and this seems essential, because of the disappearance of the filament the method becomes absolute. No material constant such as the torsion coefficient, which must be calibrated and may give rise to uncertainties, has to be taken into consideration.

The technical realization of this detection principle is coupled to the possibility of "free" rotor suspension. The magnetic suspension of ferromagnetic rotors, as used in spinning rotor vacuum gauges,[13,14] appears to be well suited. Very low and constant frictions are realized by means of this technique. By filamentless suspension the freely rotating body is also less affected by environmental shock and vibration. Moreover, frequency measurements, i.e., ultimately time measurements, appear to be more reliable than deflection measurements.

Let us discuss the quantitative aspects of the method. In a coordinate frame at rest with regard to the vacuum enclosure each area element dA of the rotor surface is moving with a tangential velocity $R\omega$ around the axis of rotation, where R is the radius of the rotor and ω the angular velocity. A molecular beam of the intensity I_0 (particles s^{-1}) is directed to the tangentially moving surface [Fig. 1(b)]. The average tangential momentum per incident molecule transferred to the rotor is $m\tilde{v}\sin\alpha$, where α is the angle of incidence with respect to the surface normal and $\tilde{v}$ the mean flow velocity of the molecular beam. In the frame of our basic assumption, i.e., scattering symmetric with respect to the surface normal, the rebounded molecules take along the tangential momentum $mR\omega$. At low rotational frequencies (e.g., 1 Hz) and finite angles α this quantity is negligible compared to the tangential momentum transferred by the impinging molecule.[15] Thus, the rotor is affected by the tangential force $F_t = I_0 m\tilde{v}\sin\alpha$, i.e., by a torque $T = I_0 m\tilde{v}\sin\alpha R$. Depending on the momentary sense of rotation, the torque causes a deceleration or an acceleration of the rotor. (In order to simplify the writing we will confine ourselves in the following to the case of rotor deceleration.) The resulting angular momentum decay $-\dot{\omega}$ is equal to the ratio of the torque over the moment of inertia of the rotor T/θ:

$$-\dot{\omega} = T/\theta. \tag{1}$$

The molecular-beam center-line intensity is obtained from

$$I_0 = -\frac{\dot{\omega}}{\omega}\theta\left(\frac{m\tilde{v}\sin\alpha R}{\omega}\right)^{-1}. \tag{2}$$

All quantities in Eq. (2) can be measured directly. The decay ratio of rotor speed $-\dot{\omega}/\omega$ is obtained from[16]

$$-\frac{\dot{\omega}}{\omega} = \frac{\tau_{n+1} - \tau_n}{\tau_{n+1}\tau_n}, \tag{3}$$

where τ_{n+1}, τ_n are successive time intervals, during which the rotor carries out a given number of revolutions. The basic advantage of this integrating time measuring procedure is the proportionality of the resolving power to τ^2 instead of the proportionality to τ.

The actual decay ratio $(\dot{\omega}/\omega)_{\text{exp}}$ consists of three terms:

$$\left(\frac{\dot{\omega}}{\omega}\right)_{\text{exp}} = \left(\frac{\dot{\omega}}{\omega}\right)_{\text{beam}} + \left(\frac{\dot{\omega}}{\omega}\right)_{GF} + \left(\frac{\dot{\omega}}{\omega}\right)_{BF}, \tag{4}$$

where $(\dot{\omega}/\omega)_{\text{beam}}$ is the beam-induced decay ratio as defined in Eq. (1), $(\dot{\omega}/\omega)_{GF}$ and $(\dot{\omega}/\omega)_{BF}$ are induced by residual gas and magnetic bearing frictions, respectively. Under high vacuum conditions ($p < 10^{-7}$ mbar) residual gas friction is negligible compared to the bearing friction.[14] Bearing frictions are mainly due to eddy currents, either induced in the sample by inhomogenities of the suspension field or in the surrounding conductors by the rotating component of the sample magnetization.[16]

According to continuum theory the flow velocity of a

supersonic nozzle beam after a distance of a few nozzle diameters, i.e., the mean velocity $\tilde{v}$, is close to the value u_{max}:

$$\tilde{v} \simeq u_{max} = \left(\frac{2\gamma}{3\gamma - 3}\right)^{1/2} \left(\frac{3kT_0}{m}\right)^{1/2}. \quad (5)$$

With Eqs. (5) and (4), Eq. (2) becomes

$$I_0 = -\theta \left[\left(\frac{\dot{\omega}}{\omega}\right)_{exp} - \left(\frac{\dot{\omega}}{\omega}\right)_{BF}\right] \left(\frac{m \sin \alpha R u_{max}}{\omega}\right)^{-1}. \quad (6)$$

Equation (5) is rigorously valid only for monatomic gases, because the conversion of the internal energy of polyatomic gases into translational energy is, in general, not complete. The conversion efficiency depends on the initial distribution of the internal energy and on the relaxation cross section. Equation (5) is only an upper limit in the case of polyatomic gas expansions. Therefore, an exact evaluation of nozzle beam intensities of polyatomic molecules involves, in addition, time-of-flight measurements for the determination of $\tilde{v}$.

The smallest decay ratio $(\dot{\omega}/\omega)_{beam}$ that can be resolved is essentially determined by δ_{BF} the standard deviation of the mean value of $(\dot{\omega}/\omega)_{BF}$ and by the ratio of the momentum of inertia over the radius of the rotor (θ/R). We take for the smallest measurable flux

$$I_0^{min} \approx 10 \delta_{BF} \theta \left(\frac{m\tilde{v} \sin \alpha R}{\omega}\right)^{-1}. \quad (7)$$

II. EXPERIMENTAL SETUP

A. General

The experimental arrangement is a modification of the time-of-flight machine used in this laboratory[17,18] for measuring the kinetic parameters of desorbing molecules: a nozzle beam unit is now added. A free jet source with a 10-μm-diam nozzle (optical) is placed 18 mm from a conical skimmer, which has a 0.29-mm-diam opening. The effective nozzle diameter is determined by total flow rate measurements, which yield a value of $d_{eff} = 7.6\,\mu$m. Before entering the scattering chamber the beam is further collimated, resulting in an angular divergence of 0.09°. The axis of the spinning rotor detector is located 568 mm downstream of the nozzle in the scattering chamber. The stagnation temperature can be varied between 10 and 800 K and is monitored with an iron–constantan or gold/iron–chromel thermocouple. The effective gas temperature in the stagnation chamber was also evaluated by means of He time-of-flight measurements.

B. Spinning rotor detector

The sectional view (Fig. 2) shows the essential parts of the spinning rotor intensity detector. The rotor consists of a 3.5-mm-diam soft iron cylinder (A) for magnetic suspension, a thin-walled aluminum connector tube (B) and, supported by a small copper screw (C), a truncated copper cone (D) with a 2-mm cylindrical rim (E). The rim on which the beam is impinging has a diameter of 30 mm. In order to reduce the moment of inertia of the system, the copper cone (and rim) wall is made as thin as possible (~0.02 mm). It still contributes 98% to θ. Good ruggedness is achieved by galvanically making it from copper and subsequent chromium plating. The overall weight of the rotor is 0.8 g and the moment of inertia 4.5×10^{-8} kg m^2.

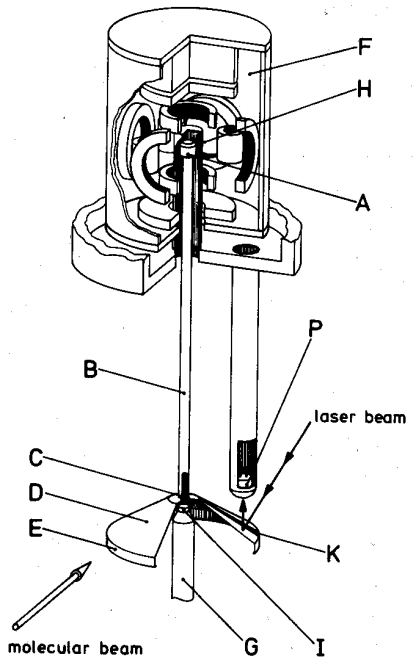

FIG. 2. Sectional view of the spinning rotor detector: (A) soft iron cylinder, (B) thin-walled aluminum tube, (C) copper screw, (D) copper cone, (E) cylindrical rim, (F) stator package, (G) supporting pivot, (H) stainless-steel tube, (I) Sm–Co permanent magnet, (K) graphite mark, (P) phototransistor.

All components for contactless suspension and for rotor acceleration are combined in a cylindrical stator package (F) outside the vacuum vessel. The stator package is taken away for baking procedures. In that case the rotor rests on the lower supporting pivot (G) while its upper part leans on a thin-walled stainless-steel tube (H) of the vacuum enclosure. Stable rotor suspension at "zero" power consumption is achieved by an active permanent magnetic suspension. The suspension, the active oscillation damping, and the drive field to bring the rotor to the coasting frequency (~1 Hz) are provided by the stator package and the corresponding control unit. Stator package and control are similar to those of the spinning rotor gauge and described in detail in the appropriate literature.[13,16] At rotational frequencies below 1.5 Hz used here an eddy current passive suppression of disturbing oscillations appeared to be effective. A small permanent magnet (I) is located on top of the supporting pivot (G). It induces eddy currents in the copper screw (C) at the lower end of the rotor when the latter is oscillating.

For the measurement of the rotational frequency a laser beam is directed on the copper cone. The reflected light enters a phototransistor (P) which is switched whenever the laser beam encounters a graphite mark (K) drawn on the cone. Since the laser beam is in the same plane with the rotor axis, the light pressure does not influence the rotor frequency. Further signal processing is shown schematically in Fig. 3. The formed signal is fed into a frequency counter giving successive durations τ_n, τ_{n+1} of rotor revolution periods. A

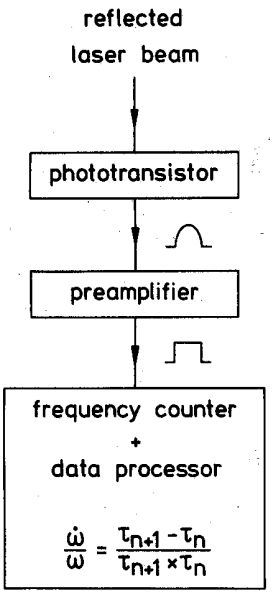

FIG. 3. Evaluation of the relative rotor deceleration rate.

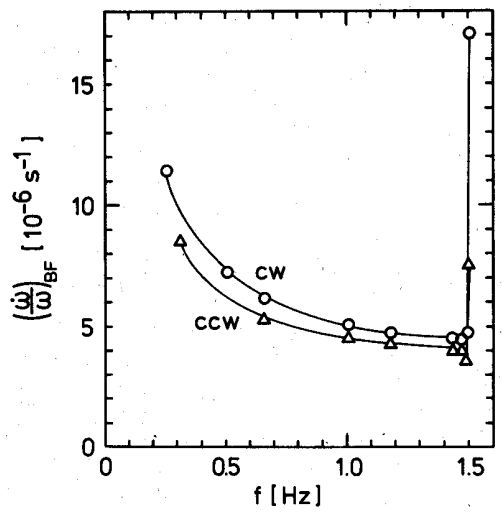

FIG. 4. Magnetic drag $(\dot{\omega}/\omega)_{BF}$ as function of the rotor frequency f; (cw) clockwise rotation, (ccw) counterclockwise rotation.

microprocessor unit calculates from these values the relative deceleration of the rotor.

C. Experimental procedure

The experimental procedure is as follows: First, the rotor is accelerated to its working frequency of 1 Hz. Then the decay ratio with the molecular beam off, i.e., the magnetic drag $(\dot{\omega}/\omega)_{BF}$ of the freely coasting rotor is determined. Subsequently the decay ratio with the molecular beam on $(\dot{\omega}/\omega)_{exp}$ is measured. Finally, the magnetic drag measurement with beam off is repeated. The measuring time for each decay ratio was $\sim$290 s. Great care has been taken to maintain the rotor at constant temperature. The laser beam heats up the rotor cone slightly, resulting in a small change in its moment of inertia. Therefore, the rotor is allowed to reach a stationary temperature with the laser on before starting the measurements.

D. Accuracy

Table I summarizes all relevant quantities which determine the accuracy of the measurement. Using the Gaussian law of propagation of errors the mean relative error is $\pm 4.5\%$.

III. RESULTS

A. Magnetic drag and sensitivity

The magnetic drag $(\dot{\omega}/\omega)_{BF}$ mainly determines the sensitivity of the detector. Two specific properties of $(\dot{\omega}/\omega)_{BF}$ are of obvious importance: the dependency on the rotor frequency and the long term variations. In Fig. 4 the residual drag for clockwise and counterclockwise rotation is shown as a function of the rotor frequency. The slight difference in the shape of the curves originates probably from a momentum of drag due to the active damping of the soft iron cylinder. The magnetic drag in Fig. 4 decreases with increasing frequency up to 1.5 Hz, where a sharp increase is obvious. A possible explanation for the decreasing drag is the existence of a momentum of stop caused by inhomogenities of the magnetic field in conjunction with small deviations of the soft iron cylinder from its rotational symmetry. At frequencies greater than 1.5 Hz the lateral passive damping at the bottom of the rotor excites a lateral rotor oscillation; the rotor gets into stagger. The long-term variations of $(\dot{\omega}/\omega)_{BF}$ are induced by mechanical or electromagnetic interferences. The magnetic drag measurement is thus performed before and after each beam drag measurement. Table II gives an example of the variation of the magnetic drag.

Taking account of the result in Fig. 4 we chose a working frequency of 1 Hz. At this frequency we achieve standard deviations of the mean $\delta_{BF} \approx 2\times10^{-8}$ s^{-1} for measuring times of $\approx$290 s. Inserting typical values in Eq. (7) ($\sin\alpha = 0.5$, $\omega = 6.28$ s^{-1}, $R = 0.015$ m, $\theta = 4.5\times10^{-8}$ kg m^2) we find the minimal measurable particle fluxes I_0^{min} for thermal nozzle beams as shown in Table III.

B. Perfect accommodation of tangential momentum

The quantitative relation between the beam intensity I_0 and the experimentally accessible values in Eq. (6) is based on the assumption that the tangential momentum of the incident molecules is perfectly accommodated upon scattering, i.e., the angular distribution of the scattered beam molecules

TABLE I. Relative errors of the various parameters in Eq. 6.

θ/R	$(\dot{\omega}/\omega)_{exp}$	$(\dot{\omega}/\omega)_{BF}$	ω	$\sin\alpha$	$\tilde{\sigma}$(Ref. 19)
1%	0.5%	0.5%	0.2%	4%	1%

TABLE II. Typical long-term variations of the magnetic drag $(\dot{\omega}/\omega)_{BF}$ at a rotor frequency of 1 Hz.

Time (h)	0	2	4	6	8	10
$(\dot{\omega}/\omega)_{BF}$($10^{-6}$ s^{-1})	4.8421	4.9211	4.7036	4.7028	4.8052	4.6917

TABLE III. Minimum measureable intensities I_0^{min} of thermal nozzle beams [Eq. (7)].

Gas \ T_0	78 K	300 K	1000 K
He	6.4×10^{11}	3.2×10^{11}	1.8×10^{11}
Ne	2.8×10^{11}	1.4×10^{11}	7.8×10^{10}
Ar	1.8×10^{11}	1.0×10^{11}	5.6×10^{10}

is symmetric with respect to the surface normal, independent of the incident angle α. This is also a prerequisite of the absolute character of the device. We will now demonstrate experimentally that the assumption is fulfilled in the limit of the present experimental errors.

It is obvious from Eq. (6) and its derivation that $[(\dot\omega/\omega)_{exp} - (\dot\omega/\omega)_{BF}]$ vs $\sin\alpha$ at constant I_0 should be a straight line only if the tangential momentum accommodation is perfect. The result of the corresponding measurements is shown in Fig. 5. Helium nozzle beams (stagnation temperature $T_0 = 304$ K) with three different intensities (stagnation pressures, p_0) are used. All data corresponding to the same beam intensity lie on straight lines. Thus, the correctness of the assumption is verified. (The slope of each line is a direct measure of the absolute beam intensity).

The result is not surprising. Thermal helium beams incident on technical surfaces, which have not been cleaned on purpose (thus probably covered with oxides and disordered absorbates) are expected to be scattered almost perfectly diffusely; other gases, of course, too. In the case of a strongly reducing environment or when using atomic hydrogen beams a renewed proof of the perfect accommodation is recommendable.

C. I_0 versus stagnation pressure

As an example for absolute He beam intensity data obtained with the spinning rotor detector, I_0 versus stagnation pressure values are presented in Fig. 6. The data are taken at fixed angle of incidence $\sin\alpha = 0.57$ and two stagnation temperatures. For comparison with other data the intensity

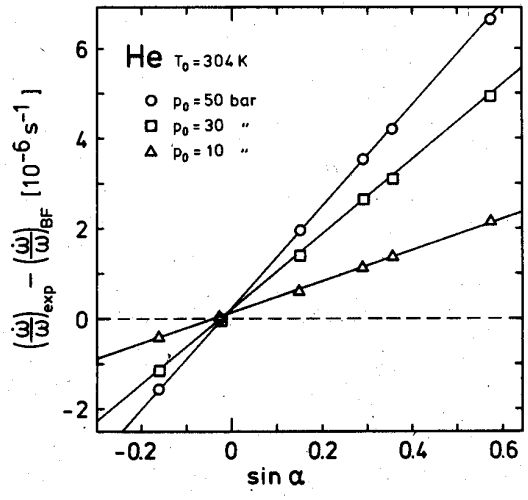

FIG. 5. Rotor deceleration $[(\dot\omega/\omega)_{exp} - (\dot\omega/\omega)_{BF}]$ vs $\sin\alpha$ at three different helium stagnation pressures, p_0.

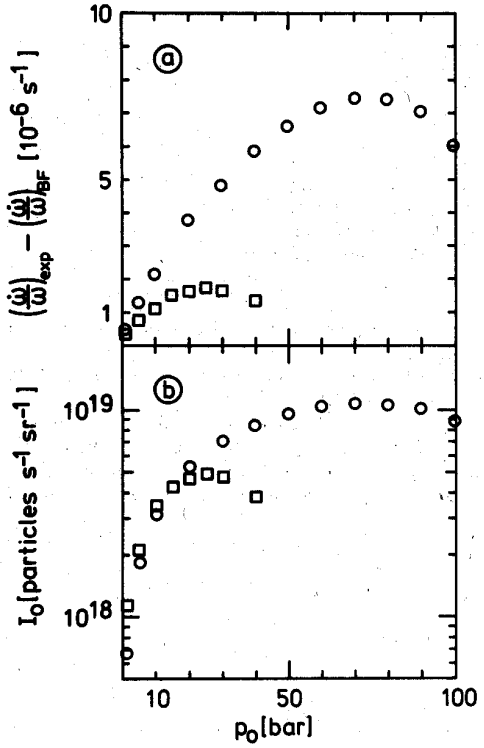

FIG. 6. (a) Measured rotor deceleration $[(\dot\omega/\omega)_{exp} - (\dot\omega/\omega)_{BF}]$ and (b) deduced absolute intensity I_0 vs stagnation He pressure p_0; stagnation temperature $T_0 = 78$ K (□) and $T_0 = 304$ K (○).

is normalized to the solid angle unit. For both stagnation temperatures the data increase with increasing pressure, reach a maximum, and decrease with further stagnation pressure increase. The maximum is reached at a nozzle chamber pressure of about 3×10^{-3} mbar. For pressures exceeding this limit residual gas scattering leads to a decrease in beam intensity.

IV. DISCUSSION

This new type of molecular-beam detector takes full advantage of the directed momentum flux of molecular beams and of the complete momentum accommodation during scattering on uncleaned surfaces and has been shown to be an absolute device. It can be used for molecules of any kind. The integral measurement of the work done by impinging beam molecules and the very low friction of the magnetic bearing are basic features for the detector abilities. The detection limit of the present design is $I_0^{min} = 1.2\times10^{15}/M\bar v$, where M is the atom mass and $\bar v$ the average velocity of the beam particles in ms^{-1}. Attempts to increase the sensitivity of the detector by minimizing the ratio of the moment of inertia to the rotor diameter and by optimizing the magnetic suspension for minimal eddy current interferences and maximal frequency resolution are in progress.

ACKNOWLEDGMENTS

The authors are grateful to Karl Veltmann for skilled technical assistance and Johan K. Fremerey for stimulating discussions.

[1]F. O. Goodman, Prog. Surf. Sci. **5**, 3 (1974).
[2]E. W. Becker and O. Stehl, Z. Angew. Phys. **4**, 20 (1952).
[3]J. G. Choi, J. S. Hayden, M. T. O'Connor, and G. J. Diebold, J. Appl. Phys. **52**, 6016 (1981).
[4]L. B. Thomas and R. G. Lord, *Rarefied Gas Dynamics* (Academic, New York, 1974), p. 405.
[5]R. G. Lord, *Rarefied Gas Dynamics* (AIAA, New York, 1977), p. 531.
[6]R. G. Lord and L. B. Thomas, Proceedings of the 7th International Vacuum Congress, edited by Dobrozemski *et al.*, Vienna, 1977, p. 1229.
[7]G. Comsa, J. K. Fremerey, and B. Lindenau, Proceedings of the 7th International Vacuum Congress, edited by Dobrozemski *et al.*, Vienna, 1977, p. 157.
[8]G. Comsa, J. K. Fremerey, and B. Lindenau, Proceedings of the 8th International Vacuum Congress, edited by Langeron and Maurice, Cannes, 1980, Vol. II, p. 218.
[9]G. Comsa, J. K. Fremerey, B. Lindenau, G. Messer, and P. Röhl, J. Vac. Sci. Technol. **17**, 642 (1980).
[10]G. Messer, Proceedings of the 8th International Vacuum Congress, edited by Langeron and Maurice, Cannes, 1980, Vol. II, p. 191.
[11]G. Messer and L. Rubet, Proceedings of the 8th International Vacuum Congress, edited by Langeron and Maurice, Cannes, 1980, Vol. II, p. 259.
[12]The minimum detectable force is given by $F_t^{\min} = (\kappa \pi r^4/2RL)$, where κ is the torsion coefficient, r the radius, and L the length of the filament, R is the disk radius. For example, if we use a quartz fiber $2r = 1\ \mu$m, $L = 20$ cm, and $\kappa = 3.2\times 10^4$ N mm^{-2} (breaking lead = 6 N), suspending a disk of $R = 15$ mm, and if we are able to measure deflections down to $\varphi = 0.01$ rad, we obtain $F_t^{\min} = 10^{-13}$ N.
[13]J. K. Fremerey and K. Boden, J. Phys. E **11**, 106 (1978).
[14]J. K. Fremerey, Vacuum **32**, 685 (1982).
[15]For a thermal helium nozzle beam ($T_0 = 300$ K) incident ($\sin\alpha = 0.5$) on a rotating disk with radius $R = 15$ mm and an angular velocity $\omega = 2\pi f = 6.28\ \text{s}^{-1}$, $m\omega R/m\bar{v}\sin\alpha = 1\times 10^{-4}$.
[16]J. K. Fremerey, Rev. Sci. Instrum. **42**, 753 (1971).
[17]G. Comsa, R. David, and B. J. Schumacher, Surf. Sci. **85**, 45 (1979).
[18]G. Comsa, R. David, and B. J. Schumacher, Rev. Sci. Instrum. **52**, 789 (1981).
[19]Even for He real gas effects cannot always be neglected: with increasing stagnation pressure, the source enthalpy increases and thus more thermal energy can be transferred into directed translational energy. Our TOF measurements show that the resulting deviation of $\bar{v}$ from $u_{\max}$ remains within $\pm 1\%$.